Electronic structure and optical properties of β-$FeSi_2$(100)/Si(001) interface at high pressure

L. Z. Liu,[1] X. L. Wu,[1,a)] X. X. Liu,[1] J. C. Shen,[1] T. H. Li,[1,2] and Paul K. Chu[3,a)]
[1]*National Laboratory of Solid State Microstructures and Department of Physics, Nanjing University, Nanjing 210093, People's Republic of China*
[2]*College of Electronic Engineering, Guangxi Normal University, Guilin 541004, People's Republic of China*
[3]*Department of Physics and Materials Science, City University of Hong Kong, Tat Chee Avenue, Kowloon, Hong Kong, China*

(Received 25 July 2012; accepted 28 August 2012; published online 13 September 2012)

The electronic structure and optical absorption properties of the β-$FeSi_2$(100)/Si(001) interface are investigated by first-principle calculation at high pressure. As the pressure increases, the optical gap decreases sharply, reaches a minimum, and then increases slowly. Structural analysis reveals that the Si(001) slab partially offsets the pressure exerted on the β-$FeSi_2$ (100) interface, thus downshifting the lowest unoccupied electronic states of the interface and decreasing the optical gap. As the pressure increases further, this offsetting effect weakens and the optical gap increases again gradually. Hence, a high pressure plays an important role in the optical behavior. © *2012 American Institute of Physics*. [http://dx.doi.org/10.1063/1.4752154]

Iron-disilicide (β-$FeSi_2$) is a semiconductor phase with a band gap of about 0.87 eV and high optical absorption coefficient of $\alpha > 10^5\,cm^{-1}$.[1–3] The two interesting characteristics make it a promising candidate in optoelectronic communication devices, near infrared detectors, solar cells, and light emitters.[4–6] In the β-$FeSi_2$/crystalline silicon heterojunction structure in a solar cell, the conversion efficiency is still too low to be practical because of the high reflectance (40%) from the interfacial layer.[7,8] Therefore, the microstructure of the β-$FeSi_2$/Si interface needs to be modified in order to enhance the photovoltaic performance. For example, traditional silicon substrates are replaced by textured ones to alter the interfacial structure, so that the β-$FeSi_2$ layer can trap light more effectively.[9] If Al is introduced into the β-$FeSi_2$/Si(100) heterojunction, the photovoltaic characteristics can also be improved significantly.[10] It has been reported that the β-$FeSi_2$/Si interface plays a crucial role in the optical properties,[11–15] but the underlying physical mechanism is not well understood. The electronic transition between the conduction band (CB) and valence band (VB) is responsible for optical absorption, and so it is of both fundamental and practical importance to determine the β-$FeSi_2$/Si interface electronic states and subsequent optical absorption behavior.

Previous electronic structure calculations conducted on β-$FeSi_2$ films indicate that the optical gap is highly sensitive to lattice distortion,[12] and a suitable stress field can alter the optical absorption band edge. When a β-$FeSi_2$ film is deposited on Si epitaxially, the diffusion rates of Fe and Si depend on the preparation methods and hence, the stoichiometry of the β-$FeSi_2$/Si interface cannot be well controlled and the interfacial layer can be largely distorted leading to further lattice mismatch.[16,17] In this respect, it is effective to apply a high pressure to simulate lattice deformation at the β-$FeSi_2$/Si interface. It is believed that if a stress field is applied to the β-$FeSi_2$/Si interface, optical absorption can be altered due to changes in the structure and electronic state. Therefore, a systematic investigation of the electronic states and optical behavior of the β-$FeSi_2$/Si interface at high pressure are important. In this work, we theoretically investigate the changes in the optical absorption and structures of the β-$FeSi_2$/Si interface at different pressure.

The heteroepitaxial system consisting of the β-$FeSi_2$ (100)/Si(001) interfacial structure[14] is studied. The calculation is based on the density functional theory (DFT) in generalized gradient approximation (GGA) and Perdew-Burke-Ernzerhof (PEB) exchange-correlation potential, using the CASTEP package with Norm-conserving pseudopotentials.[18,19] The Fe $3d^64s^2$ orbitals and Si $3s^23p^2$ orbitals are treated as valence states. An energy cutoff of 500 eV is used to expand the plane wave functions. The β-$FeSi_2$ (100)/Si(001) interfacial layer is considered to comprise twelve layers of β-$FeSi_2$ (100) and a Si (001) slabs, as shown in Fig. 1(a) and it has been verified to be well converged. The corresponding film structure is modeled by a β-$FeSi_2$ primitive cell. A Monkhorst Pack k-points grid is $2 \times 2 \times 1$ for the β-$FeSi_2$ (100)/Si(001) slab and $2 \times 2 \times 2$ for the β-$FeSi_2$ primitive cell. The bottom two layers are fixed to mimic the bulk structure, and relaxation is performed until the following convergence tolerances: 1×10^{-5} eV for energy, 0.03 eV/Å for maximum force, and 0.001 Å for maximum displacement. An external stress is applied by equivalent hydrostatic pressure, and the optical properties are calculated based on the independent-particle approximation. The imaginary part of the dielectric function due to transitions between the occupied and unoccupied electronic states is given by the Fermi golden rule,[20]

$$\varepsilon(\hbar\omega) = \frac{2e^2\pi}{\Omega\varepsilon_0}\sum_{\vec{k},v,c}\left|\langle\psi^c_{\vec{k}}(\vec{r})|\,\vec{u}\cdot\vec{r}|\psi^v_{\vec{k}}(\vec{r})\rangle\right|^2 \times\delta\left(E^c_{\vec{k}} - E^v_{\vec{k}} - \hbar\omega\right),$$

where Ω is the slab unit-cell volume, $\hbar\omega$ is the photon energy, $\vec{k}$ is the Bloch wave vector, $E^{c(v)}_{\vec{k}}$ and $|\psi^{c(v)}_{\vec{k}}(\vec{r})>$ are

a)Authors to whom correspondence should be addressed. Electronic addresses: hkxlwu@nju.edu.cn and paul.chu@cityu.edu.hk.

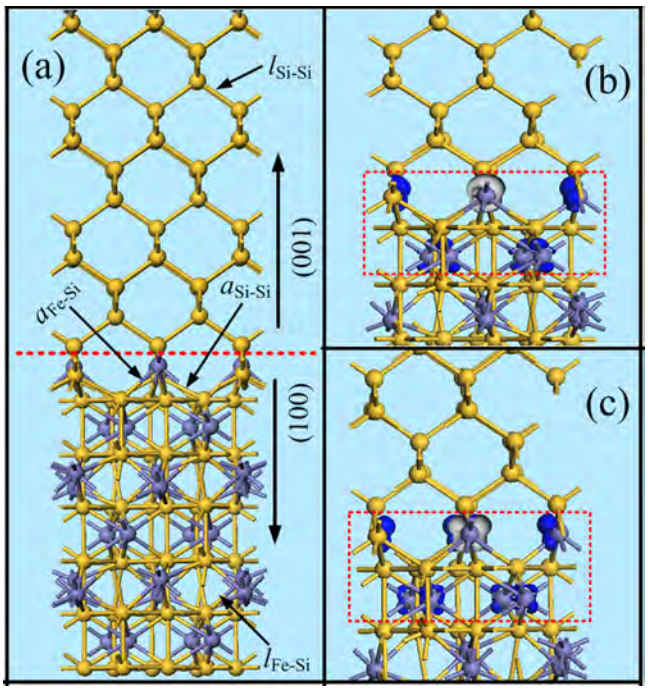

FIG. 1. (a) Atomic configuration in the β-$FeSi_2$ (100)/Si(001) model. The interfacial layer is marked by the red dash line, the crystal orientations are marked by arrow, and gray and yellow balls represent Fe and Si atoms, respectively. The Fe-Si and Si-Si bonds at the interfacial ($a_{Fe\text{-}Si}$ and $a_{Si\text{-}Si}$) and interior regions ($l_{Fe\text{-}Si}$ and $l_{Si\text{-}Si}$) are also marked. The isosurfaces for electronic orbitals of the highest occupied state and lowest unoccupied state at pressure P = 0 GPa are displayed in (b) and (c), respectively.

the eigen-energy and wave function, where the superscripts c and v denote the states in CB and VB, respectively, $\vec{r}$ is the position vector, and $\vec{u}$ is the unit vector along the light polarization. The absorption coefficient can be obtained by: $\alpha = \frac{2\varepsilon(\hbar\omega)\hbar\omega}{c}$; here, c is the light velocity.

To test the validity of our model, the structural parameters of β-$FeSi_2$ calculated by the CASTEP package using previous theoretical and experimental results are compared in Table I. The lattice constants (a, b, and c) and optical band (E_g) obtained from CASTEP calculations are 9.847, 7.782, 7.838 Å, and 0.787 eV, which are smaller than previous experimental results,[21] but better than those derived by *ab initio* density-functional calculation.[14] With regard to the linear muffin-yin orbital (LMTO) calculation,[12] when the lattice constants are consistent with experimental values, the calculated optical gap is only 0.760 eV. Hence, it can be inferred that our calculation results are better than those of previous ones, although there are inevitable underestimation in the optical gaps.

The absorption spectra of β-$FeSi_2$ (100)/Si(001) slabs at pressure P of 0, 2, 3, 4, 6, and 8 GPa are calculated and shown in Fig. 2(a). The absorption edges unexpectedly

TABLE I. Structural parameters and optical bandgaps calculated using the CASTEP package, *ab initio* density-functional theory, and LMTO methods. The last two columns show the experimental results.

	CASTEP	*ab initio* (Ref. 14)	LMTO (Ref. 12)	Expt. (Ref. 12)
a (Å)	9.847	9.825	9.863	9.863
b (Å)	7.782	7.736	7.791	7.791
c (Å)	7.838	7.920	7.833	7.833
E_g (eV)	0.787	0.730	0.760	0.875

downshift from P = 0 to 2 GPa in the beginning and then upshift from P = 3 to 8 GPa. This behavior is different from previous results obtained from β-$FeSi_2$ films[13] showing that the absorption edges upshift monotonically with increasing pressure. To further assess this optical behavior, the optical gaps are obtained by $\alpha = \frac{A}{\hbar\omega}(\hbar\omega - E_g)^{\beta}$, and the calculated results are shown in Fig. 2(b). Here, A is the constant including the square of the photon energy independent optical dipole matrix element, $\hbar\omega$ is the photon energy, E_g is the optical gap, and β is the parameter for the joint density of states (DOS).[13,22] The calculated results show that the optical gap decreases sharply with increasing pressure initially, reaches a minimum at about P = 2 GPa, and then begins to increase slowly. To elucidate the physical origin, the corresponding results of only a β-$FeSi_2$ film are also calculated and shown in Fig. 2(c). A significant linear relationship can be observed between the optical gap and applied pressure and this behavior is in agreement with previous experimental data.[13] Neglecting the underestimation in the DFT calculation, an obvious different behavior is observed from Figs. 2(b) and 2(c). In addition, the optical gap of the β-$FeSi_2$ (100)/Si(001) slab is obviously smaller than that of the β-$FeSi_2$ film, and it can be ascribed to the interfacial states introduced to the band gap of the β-$FeSi_2$ film. Hence, it can be inferred that this optical behavior is related to the complex β-$FeSi_2$ (100)/Si(001) interfacial structure. Owing to the different elastic constants, different deformation at a high pressure between the Si and β-$FeSi_2$ interfacial and internal regions are considered naturally to interpret the physical phenomenon.

To confirm our hypothesis, the electronic DOS of the β-$FeSi_2$ (100)/Si(001) interface and β-$FeSi_2$ film are shown in Figs. 3(a) and 3(c) in which the red dashed line represents the highest occupied electronic state. In the β-$FeSi_2$ film [Fig. 3(a)], the DOS peak (P_0) at CB upshifts slightly when pressure is applied. To make it more clear, the DOS edges (marked by S_1) are magnified and shown in Fig. 3(b). The energies of the lowest unoccupied states increase from 0.79 to 0.91 eV, which will enlarge the transition energy between the highest occupied and lowest unoccupied electronic states. This can explain the linearly increasing optical gap of the β-$FeSi_2$ film with increasing pressure. Compared to the DOS of β-$FeSi_2$ film, the β-$FeSi_2$ (100)/Si(001) interface not only

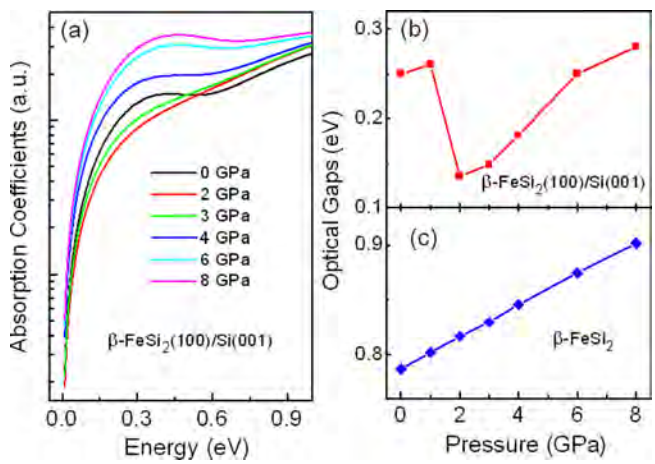

FIG. 2. (a) Calculated absorption spectra of the β-$FeSi_2$ (100)/Si(001) slab at pressure P of 0, 2, 3, 4, 6, and 8 GPa. (b) Calculated optical bandgap of the β-$FeSi_2$ (100)/Si(001) slab. (c) Calculated optical gap of the β-$FeSi_2$ film.

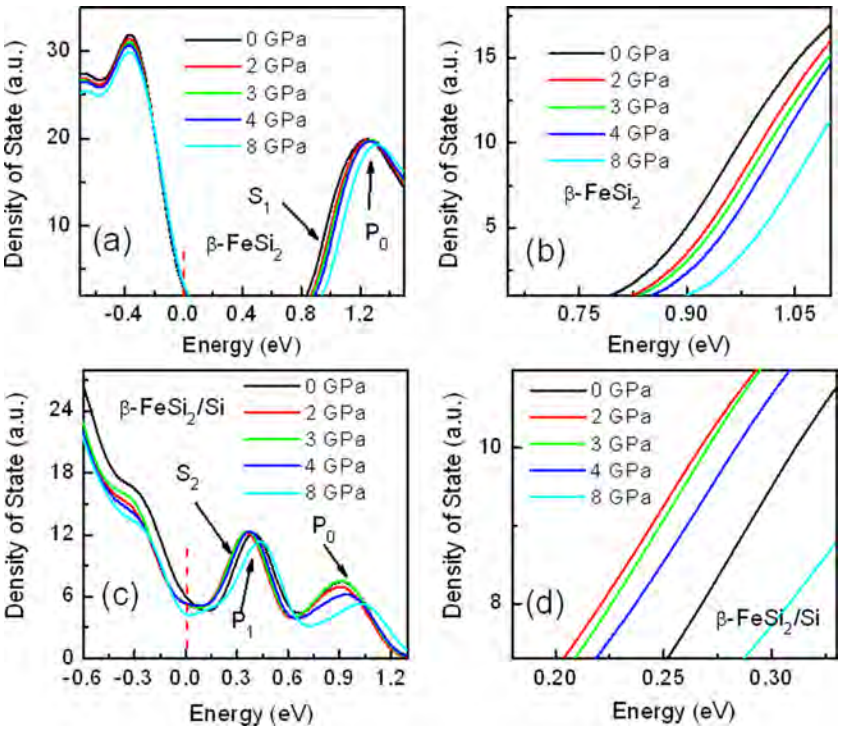

FIG. 3. Calculated densities of states (DOSs) of (a) β-$FeSi_2$ film and (c) β-$FeSi_2$ (100)/Si(001) slab at pressure P = 0, 2, 3, 4, and 8 GPa. The corresponding DOS peak edges (marked by S_1 and S_2) of the β-$FeSi_2$ film and β-$FeSi_2$ (100)/Si(001) slab are magnified and shown in (b) and (d), respectively.

introduces the P_1 state arising from the heterojunction interface but also downshifts the original P_0 state, as shown in Fig. 3(c). The optical bandgap of the β-$FeSi_2$ (100)/Si(001) interface becomes obviously smaller than that of the β-$FeSi_2$ film. As the pressure increases, the two sub-peaks (P_1 and P_0) initially downshift (at P = 2) and then upshift (at P = 3, 4, and 8 GPa). Correspondingly, the electronic transition energy first decreases and then increases gradually. To clearly demonstrate this behavior, the interfacial state DOS edge (marked by S_2) is also magnified and depicted in Fig. 3(d). The lowest unoccupied state diminishes sharply to 0.21 eV at P = 2 GPa, increases slowly at P = 3, 4 GPa, and finally exceeds 0.25 eV at P = 0 GPa reaching 0.28 eV at P = 8 GPa. This trend is in good agreement with the optical bandgap change illustrated in Fig. 2(b). The results clearly indicate that the distributions of DOSs can be affected by the high pressure and explains why the β-$FeSi_2$ (100)/Si(001) interface exhibits different optical absorption properties.

To further study the DOS changes, we examine the distributions of the electronic states at the VB and CB by orbital analysis. Our calculation shows that under different applied high pressure, the electronic orbital distributions are only modified slightly, but the main features are the same. The electronic orbital analysis of the highest occupied states and lowest unoccupied states at pressure P = 0 GPa are displayed in Figs. 1(b) and 1(c), respectively. The electronic states are dispersed in the regions of the interfacial Fe atom orbitals (marked by red rectangle), but slightly located at the internal Fe and Si atom orbitals. This implies that the absence of some Si atoms at the interface does not affect optical absorption significantly. Our calculations conducted for silicon vacancies at different locations also confirm this point (data not shown here). These results disclose that the two β-$FeSi_2$ atomic layers in the interfacial region are mainly responsible for the optical absorption and, therefore, the interfacial lattice distortion as a result of a higher pressure can explain the optical absorption behavior.

To illustrate the structural distortion, the calculated structural parameters of the β-$FeSi_2$ (100)/Si(001) slab, β-$FeSi_2$, and Si films are shown in Table II. The lengths of

TABLE II. Structural parameters at high pressure calculated using the CASTEP package. The Fe-Si and Si-Si bond lengths determined from the β-$FeSi_2$ (100)/Si(001) slab at the interfacial ($a_{Fe\text{-}Si}$ and $a_{Si\text{-}Si}$) and internal regions ($l_{Fe\text{-}Si}$ and $l_{Si\text{-}Si}$) are listed in the first half to compare the difference (ΔL). The deformation $[(V_p - V_0)/V_0]$ of the β-$FeSi_2$ and Si films and the differences ($\Delta\varepsilon$) are listed in the second half with the last two columns showing the elastic constants (C_{44}) of β-$FeSi_2$ and Si.

	Fe-Si bond (Å)			Si-Si bond (Å)			$(V_p-V_o/V_o(\%)$			C_{44}(GPa)	
P (GPa)	Interfacial	Internal	ΔL (Å)	Interfacial	Internal	ΔL (Å)	$FeSi_2$	Si	Δε (%)	$FeSi_2$	Si
0.0	2.297	2.385	0.088	2.342	2.355	0.013	0.00	0.00	0.00	127.1	80.31
1.0	2.288	2.379	0.091	2.340	2.354	0.014	0.57	1.04	0.47	129.7	80.33
2.0	2.275	2.375	0.100	2.319	2.348	0.029	1.13	2.03	0.90	133.2	81.71
2.5	2.274	2.373	0.099	2.319	2.342	0.023	1.38	2.50	1.12	133.9	81.95
3.0	2.273	2.371	0.098	2.318	2.334	0.016	1.65	2.96	1.31	135.3	81.96
4.0	2.269	2.366	0.097	2.312	2.324	0.012	2.18	3.85	1.67	136.8	82.40
6.0	2.266	2.357	0.091	2.306	2.318	0.012	3.21	5.55	2.34	141.7	82.77
8.0	2.263	2.346	0.083	2.288	2.299	0.011	4.16	7.10	2.94	144.7	84.48

the Fe-Si and Si-Si bonds at the interface ($a_{Fe\text{-}Si}$, $a_{Si\text{-}Si}$) and interior ($l_{Fe\text{-}Si}$, $l_{Si\text{-}Si}$) are compared [($a_{Fe\text{-}Si}$, $a_{Si\text{-}Si}$) and ($l_{Fe\text{-}Si}$, $l_{Si\text{-}Si}$) are marked in Fig. 1(a)]. As the pressure increases, the lengths of the Fe-Si and Si-Si bonds decrease linearly, but the $a_{Fe\text{-}Si}-a_{Si\text{-}Si}$ and $l_{Fe\text{-}Si}-l_{Si\text{-}Si}$ values increase initially reaching a maximum and then decreases gradually. The change in the bond length is similar to that of the bandgap alternation at a high pressure. On account of the different elastic coefficients C_{44} (last columns in Table. II), the Si(001) slab may partially offset the pressure exerted onto the β-$FeSi_2$ (100) slab thereby increasing the difference in the bond lengths. As the pressure is further increased, the compressed Si(001) slab cannot offset effectively the applied pressure and consequently, the bond length difference decreases slowly. This special transformation in the interfacial region causes the electronic state distributions and electronic transition energy to change. Finally, the optical properties are modified [Fig. 2(b)]. In the single β-$FeSi_2$ and Si films, the deformation and deformation difference increase monotonically as consistent with the calculated results in Fig. 2(c). This explains why the β-$FeSi_2$ (100)/Si(001) interface and β-$FeSi_2$ film exhibit significantly different optical behavior, and our study discloses that this phenomenon can be attributed to the deformation caused by different pressure.

In summary, as the pressure increases, the absorption spectra theoretically derived from the β-$FeSi_2$ (100)/Si(001) slab indicate that the optical gap decreases initially, reaches a minimum, and then increases gradually. Structural analysis and electronic state density calculation disclose that the Si(001) slab partially offsets the pressure exerted onto the β-$FeSi_2$ (100) surface, and so the lengths of the Fe-Si and Si-Si bonds at the interface are larger than those in the internal region. This is equivalent to strain applied to the interfacial region. It causes the lowest unoccupied electronic state at the DOS peak (P_1) edge to downshift and meantime the optical gap becomes smaller. As the pressure increases further, the compressed structure cannot offset effectively the high pressure. The bond length difference decreases and finally, the optical gap increases slowly. Our results reveal that the electronic structure and optical properties of the β-$FeSi_2$ (100)/Si(001) interface are obviously different from those of the β-$FeSi_2$ film, and a high pressure plays a crucial role in the optical adsorption. This phenomenon needs to be considered in device design particularly pertaining to photovoltaic applications.

This work was jointly supported by Grants (Nos. 2011CB922102 and 60976063) from the National Natural Science Foundation and Basic Research Programs of China, and Postdoctoral Science Foundation of China and Jiangsu Province (2011M500889 and 1102001B). Partial support was also from PAPD and Hong Kong Research Grants Council (RGC) General Research Fund (GRF) No. CityU 112510.

[1]K. Noda, Y. Terai, S. Hasimoto, K. Yoneda, and Y. Fujiwara, Appl. Phys. Lett. **94**, 241907 (2009).
[2]D. Leong, M. Harry, K. J. Reeson, and K. P. Homewood, Nature (London) **387**, 686 (1997).
[3]K. Yamaguchi and K. Mizushima, Phys. Rev. Lett. **86**, 6006 (2001).
[4]D. H. Tassis, C. L. Mitsas, T. T. Zorba, C. A. Dimitriadis, O. Valassiades. D. I. Siapkas, M. Angelakeris, P. Poulopoulos, and N. K. Flevaris, J. Appl. Phys. **80**, 962 (1996).
[5]J. Tani, M. Takahashi, and H. Kido, Physica B **405**, 2200 (2010).
[6]M. Ito, H. Nagai, E. Oda, S. Katsuyama, and K. Majima, J. Appl. Phys. **91**, 2138 (2002).
[7]Y. Makita, Y. Nakayama, Y. Fukuzawa, S. N. Wang, N. Otogawa, Y. Suzuki, Z. X. Liu, M. Osamura, T. Ootsuka, T. Mise, and H. Tanoue, Thin Solid Films **461**, 202 (2004).
[8]T. Ootsuka, Z. X. Liu, M. Osamura, Y. Fukuzawa, R. Kuroda, Y. Suzuki, M. Otogawa, T. Mise, S. N. Wang, Y. Hoshino, Y. Nakayama. H. Tanoue, and Y. Makita, Thin Solid Films **476**, 30 (2005).
[9]J. X. Xu, R. H. Yao, and Y. R. Liu, Appl. Surf. Sci. **257**, 10168 (2011).
[10]G. K. Dalapati, S. L. Liew, A. S. W. Wong, Y. Chai, S. Y. Chiam, and D. Z. Chi, Appl. Phys. Lett. **98**, 013507 (2011).
[11]D. N. Leong, M. A. Harry, K. J. Resson, and K. P. Homewood, Appl. Phys. Lett. **68**, 1649 (1996).
[12]L. Miglio, V. Meregalli, and O. Jepsen, Appl. Phys. Lett. **75**, 385 (1999).
[13]K. Takarabe, R. Teranishi, J. Oinuma, and Y. Mori, Phys. Rev. B **65**, 165215 (2002).
[14]S. J. Clark, H. M. Al-Allak, S. Brand, and R. A. Abram, Phys. Rev. B **58**, 10389 (1998).
[15]J. I. Tani, M. Takahashi, and H. Kido, Intermetallics **18**, 1222 (2010).
[16]T. Miki, Y. Matsui, Y. Teraoka, Y. Ebina, K. Matsubara, and K. Kishimoto, J. Appl. Phys. **76**, 2097 (1994).
[17]Z. X. Liu, M. Tanaka, R. Kuroda, M. Osamura, and Y. Makita, Appl. Phys. Lett. **93**, 021907 (2008).
[18]D. R. Hamann, M. Schluter, and C. Chiang, Phys. Rev Lett. **43**, 1494 (1979).
[19]J. P. Perdew, K. Burke, and M. Ernzerhof, Phys. Rev Lett. **77**, 3865 (1996).
[20]S. Ju and T. Y. Cai, Appl. Phys. Lett. **93**, 251904 (2008).
[21]P. Y. Dusausoy, J. Protas, R. Wandji, and B. Roques, Acta Crystallogr., Sect. B: Struct. Crystallogr. Cryst. Chem. **27**, 1209 (1971).
[22]F. Wooten, *Optical Properties of Solids* (Academic, New York, 1972), p. 115.